Numerical simulation of the dynamical properties of the human tympanum

E. Alvarado-Anell and M. Sosa*
Instituto de Física, Universidad de Guanajuato,
Apartado Postal E-143, 37000 León, Gto., México.

M.A. Moreles
Centro de Investigación en Matemáticas,
Apartado Postal 402, 36240 Guanajuato, Gto., México.

A numerical simulation of the dynamical properties of the tympanic membrane is presented. A simple and different simulation of the vibratory patterns of the coupled system of the tympanum-malleus have been assessed by proposing the modeling of the tympanum through the vibrations of a forced elastic membrane, whereas the effect of the manubrium is introduced through a forced semi-membrane. We propose the superposition of these waveforms as a model for describing the vibrations of the coupled system of the tympanum-malleus. Both waveforms have analytical representations leading to simple computations. The results of the simulation for the vibrational mode (1,1) show an amplitude for the membrane larger than those for the handle of the malleus. The maximum amplitude obtained was around 1 μm, at a test frequency of 2 kHz. Also, level curves corresponding to the simulated vibrational modes were obtained. The numerical model presented can be easily handled to change input parameters, such as sound pressure and frequency. Also, other situations such as the conical shape of the tympanum or some asymmetries could be considered.

Keywords: Tympanum-malleus system; membrane vibrations; forced semi-membrane.

Una simulación numérica de las propiedades dinámicas de la membrana timpánica es presentada. Un método simple y distinto de simulación de los patrones de vibración del sistema acoplado tímpano-martillo ha sido evaluado proponiendo la modelación del tímpano a través de las vibraciones de una membrana elástica forzada, en tanto que el efecto del mango del martillo es introducido a través de una semi-membrana. Se propone la superposición de estos dos estados como un modelo para describir las vibraciones del sistema acoplado tímpano-martillo. Ambas soluciones tienen representaciones analíticas que llevan a cálculos computacionales simples. Los resultados de la simulación para el modo vibracional (1,1) muestran una amplitud para la membrana mayor que aquella para el mango del martillo. La máxima amplitud obtenida fue de aproximadamente 1 μm, a una frecuencia de prueba de 2 kHz. Además, curvas de nivel correspondientes a los modos vibraciones simulados fueron obtenidos. El modelo numérico presentado puede ser fácilmente manipulado para cambiar los parámetros de entrada, tales como la presión y frecuencia del sonido. Así mismo, otras situaciones tales como la forma cónica del tímpano o algunas asimetrías pudieran ser consideradas.

Descriptores: Sistema tímpano-martillo; vibraciones de membrana; semi-membrana forzada.

PACS: 01.55; 02.70; 87.15.Aa

1. Introduction

The study of the dynamics of the human tympanic membrane (TM) is essential for a better understanding of the hearing mechanism of the middle ear (ME). Experimental methods for studying the TM vibrations and the sound transmission through the normal ME have been performed on temporal bones in human cadaveric and animals, by using different experimental procedures. Simultaneously, computerized theoretical modeling of the human ME have been extensively carried out. Several pathological conditions such as stiffness, fixation of the ossicular chain, chain disarticulation, etc., have been also analyzed.

In recent years, finite-element models (FEM) of the ME have become generally used, due in part to the modern computational power and the feasibility of this technique of modeling very complex systems such as the ME.

Three-dimensional FEMs of the ME including the TM, external auditory meatus, ossicular chain, ME cavity and ME ligaments and muscles, and also morphologic data and boundary conditions have been developed [1-5].

Several FEMs have particularly emphasized the role of both the geometric and mechanical properties of the TM and the coupling of the manubrium on the eardrum. Bornitz *et al.* [6] used a FEM of the human ME for parameter estimation of the TM, by comparison of the natural frequencies and mode shapes of the TM between the model and the specimens. Drescher *et al.* [7] studied the geometric properties of a human cadaver TM specimen and its coupling with the malleus by using a finite shell model. The mechanical coupling between the TM and the manubrium was also investigated by Funnell [8]. He demonstrated the critical role of curvature in the behavior of the eardrum. Mechanical properties of the manubrium were examined by Funnell *et al.* [9] by using a FEM of a cat eardrum. They found that a significant degree of manubrial bending occurs in the model. Lesser and Williams [10] applied FEMs in a two-dimensional cross-sectional model of the TM and the malleus. The shape of the displaced TM was found to be sensitive to several factors such as the elastic modulus of the membrane and the presence and position of the rotation of the malleus. Also, Decraemer

and Khanna [11] found that the description of the motion of the cat manubrium requires a rotational and a translational component, instead of a pure rotation, as classically assumed.

Several studies, both experimental and theoretical, have reported the importance that some parameters of the TM such as shape [12-14], surface structure [15], mechanical properties [16] and distributed acoustical load [17], and also ME cavity [18] and ME impedance [19], have for a better transmission of vibrations from the eardrum to the ME.

Other descriptions of the ME including analog circuit models [20,21] and lumped parametric models [22] have been developed.

Most of these studies agree that the TM is a complex structure, in which one of the main challenges for its modeling is probably the coupling to the malleus.

In this paper a simple and different modeling of the TM including the coupling to the malleus is presented. Vibrations of a forced elastic membrane model the TM, whereas the effect of the manubrium is introduced through a forced semi-membrane. We propose the superposition of these waveforms as a model for vibrations of the coupled system of the tympanum-malleus. Both waveforms have analytical representations leading to simple computations. Vibrations of this system correspond satisfactorily to that observed experimentally for the TM.

2. The mathematical model

2.1. Circular elastic membrane

Let an elastic membrane occupy D, the disk of radius b centered at the origin, and let C its boundary. A model for vibrations of this type of elastic membrane is the wave equation

$$\frac{\partial^2 u}{\partial t^2} = c^2 \nabla^2 u + w\,(x, y, t); \quad (x, y, t) \in D \times [0, +\infty), \quad (1)$$

subject to initial conditions

$$u\,(x, y, 0) = f\,(x, y), \quad \frac{\partial u}{\partial t}\,(x, y, 0) = g\,(x, y);$$

$$(x, y) \in D. \quad (2)$$

In (1), $w\,(x, y, t)$ is the forcing term and $c^2 = T/\rho$, where T is the tension and ρ the density, both assumed to be constants. If the membrane is fixed at C, the following boundary condition holds:

$$u\,(x, y, t) = 0; \quad (x, y, t) \in C \times [0, +\infty). \quad (3)$$

Solving the initial-boundary value problem (IBVP) (1)-(3), we are led to the solution

$$u\,(x, y, t) = \sum_{n=0}^{\infty} \sum_{k=1}^{\infty} \left(u_{n,k}\,(t)\,\Phi_{n,k}\,(r, \theta) \right.$$

$$\left. + U_{n,k}\,(t)\,\Psi_{n,k}\,(r, \theta) \right), \quad (4)$$

where $\Phi_{n,k}\,(r, \theta)$ and $\Psi_{n,k}\,(r, \theta)$ are the vibration modes. The functions $u_{n,k}\,(t)$ and $U_{n,k}\,(t)$ satisfy the equation $T''\,(t) + c^2 \mu^2 T\,(t) = 0$, with an inhomogeneous right-hand side.

2.2. Vibration of a semi-membrane

By cutting a sector of angle α, $0 \leq \alpha < 2\pi$ a semi-membrane is obtained. It occupies the domain

$$D_\alpha = \{(r, \theta) : 0 \leq r \leq b, \alpha \leq \theta \leq 2\pi\}.$$

Now, we consider (1) and (2) for a function $s\,(x, y, t)$ and replace condition (3) by

$$s\,(x, y, t) = 0; \quad (x, y, t) \in \partial D_\alpha \times [0, +\infty). \quad (5)$$

We observe that in D_α the function $\Theta\,(\theta)$ is no longer 2π-periodic. After some algebra we get

$$\Theta_n\,(\theta) = \sin \frac{n\pi}{2\pi - \alpha}\,(\theta - \alpha), \quad n = 1, 2, 3, \ldots \quad (6)$$

Therefore, the modes of vibration for a semi-membrane are

$$F_{n,k}\,(r, \theta) = J_{\nu n} \left(\frac{\delta_{n,k}}{b} r \right) \sin \frac{n\pi}{2\pi - \alpha}\,(\theta - \alpha),$$

$$n = 1, 2, 3, \ldots \quad (7)$$

where J_ν is the Bessel function of order ν.

So, the solution of the IBVP (1), (2) and (5) can be written in the form

$$s\,(x, y, t) = \sum_{n=1}^{\infty} \sum_{k=1}^{\infty} s_{n,k}\,(t)\,F_{n,k}\,(r, \theta), \quad (8)$$

where the function F is just as defined in (2.7). As before, $s_{n,k}$ satisfies the equation $T''\,(t) + c^2 \mu^2 T\,(t) = 0$, with an inhomogeneous right-hand side.

2.3. A model for vibration of the TM

We assume that a circle is a good approximation to the actual geometry of the TM, as can be seen from Figure 1. Under this assumption, it is reasonable to consider radial data. Thus, considering that the initial conditions $f\,(x, y)$, $g\,(x, y)$ and the source term $w\,(x, y, t)$ are independent of θ, namely $f\,(x, y) \equiv f\,(r), g\,(x, y) \equiv g\,(r)$, and $w\,(x, y, t) \equiv w\,(r, t)$ then Eq. (4), which represents the solution of the membrane, becomes

$$u\,(x, y, t) = \sum_{k=1}^{\infty} u_{0,k}\,(t)\,\Phi_{0,k}\,(r),$$

where only the terms with $n = 0$ are non-trivial. Hence, assuming the representations

$$f\,(r) = \sum_{k=1}^{\infty} f_k \Phi_{0,k}\,(r), \quad g\,(r) = \sum_{k=1}^{\infty} g_k \Phi_{0,k}\,(r),$$

and

$$w\left(r,t\right) = \sum_{k=1}^{\infty} w_k\left(t\right) \Phi_{0,k}\left(r\right),$$

where

$$f_k = \frac{1}{\int_D \left(\Phi_{0,k}\right)^2} \int_D f\Phi_{0,k}$$

and similarly for $g\left(r\right)$ and $w\left(r,t\right)$, the solution becomes

$$s\left(x,y,t\right) = \sum_{n=1}^{\infty}\sum_{k=1}^{\infty} s_{2n-1,k}\left(t\right) F_{2n-1,k}\left(r,\theta\right). \quad (9)$$

A model for vibration of the TM is the superposition of the waveforms (9) and (9).

2.4. Superposition of leading modes

It is well known that in linear elastic systems, the leading term represents satisfactorily the vibration of the whole system. In light of this, the model we propose is the superposition of the leading terms in (9) and (9).

In polar coordinates, vibrations of the TM are represented by

$$z\left(r,\theta,t\right) = u_{0,1}\left(t\right) J_0\left(\frac{\lambda_{0,1}}{b}r\right)$$
$$+ s_{1,1}\left(t\right) J_{1/2}\left(\frac{\delta_{1,1}}{b}r\right)\sin\frac{1}{2}\theta. \quad (10)$$

To derive an explicit expression of $z\left(r,\theta,t\right)$, let us specify the initial data and source term. In the absence of sound, the equilibrium position of the TM is shaped as a cap with a rather small curvature (see Fig. 1). Hence, the initial deformation of the circular membrane is taken of the form $f\left(r\right) = m\left(b^2 - r^2\right)$, with $m = 0.05$ corresponding to the natural shape of the tympanum. Vibration is a result of sound, which is external. Consequently, the initial velocity is zero, $g\left(r\right) \equiv 0$.

For the source term, $w\left(r,t\right)$, a periodic pressure of the form $P_0 \sin\omega t$ is considered. Here, P_0 is a constant pressure determined by both the intensity and the frequency ω of the sound that impinges on the tympanum. With regard to the semi-membrane, the source term is that of the membrane. Furthermore, we assume that it begins at rest: $f\left(r\right) \equiv 0, g\left(r\right) \equiv 0$.

During vibration, the coupling to the malleus manifests itself as a damping mechanism in the area surrounding it, where vibrations are significantly smaller. We shall see that simulations of (10) model this behaviour satisfactorily.
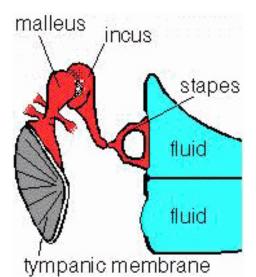

FIGURE 1. A simple diagram of the middle ear anatomy, showing the tympanic membrane and the malleus.

2.5. Model parameters

The small deflection $w\left(x,y\right)$ of a thin membrane under uniform tension T, fixed to a boundary C and subject to a net uniform pressure p, satisfies

$$\nabla^2 w\left(x,y\right) \equiv \frac{\partial^2 w\left(x,y\right)}{\partial x^2} + \frac{\partial^2 w\left(x,y\right)}{\partial y^2} = -\frac{p}{T}.$$

Here w is taken to be positive or "upward" in the direction of increasing z, and p is the excess of upward pressure over downward pressure.

Let us introduce a procedure to estimate T. Recall that for a function $\varphi\left(x\right)$ the curvature $\kappa\left(x\right)$ is defined by

$$\kappa\left(x\right) = \frac{|\varphi''\left(x\right)|}{\left[1 + \left(\varphi'\left(x\right)\right)^2\right]^{3/2}}; \quad (11)$$

notice that if $\varphi'\left(x\right)$ is small, then $\kappa\left(x\right) \approx |\varphi''\left(x\right)|$.

Let the membrane occupy the disc D of radius b, centered at $(0,0)$. Assume that the deflection $w\left(x,y\right)$ is spherical, and $w_0 = w\left(0,0\right)$ is known. Also

$$\frac{\partial^2 w\left(0,0\right)}{\partial x^2} = \frac{\partial^2 w\left(0,0\right)}{\partial y^2}.$$

Because w_0 is small, we can approximate the tension T from the equation $2\kappa_0 = \frac{P}{T}$, where κ_0 is the curvature of the circle passing through the points $(-b, 0)$, $(0, w_0)$, $(b, 0)$ and κ_0 is the reciprocal of the radius of curvature r, that is $\kappa_0 = 1/r$; then it is readily seen that

$$r = \frac{1}{2}\left(b + \sqrt{b^2 + 2\left(w_0^2 + b^2\right)}\right). \quad (12)$$

3. Numerical simulation

In Sec. 2 we got a mathematical model to describe the behaviour of the coupled system of the tympanum-malleus. For

the simulation we consider a membrane of radius $b = 0.5$ cm, which is approximately that of the tympanum and a sound frequency $\omega = 2$kHz, which corresponds to the range commonly employed in several tests. The pressure of the sound wave used was in the range determined by the minimum audible pressure, 2×10^{-5} Pa, and the maximum one, 20 Pa, just when pain starts to appear. Maple 5.0 and Mathematica 8.0 softwares were employed.

From (10), expressions for $s_{1,1}(t)$ and $u_{0,1}(t)$ can be found to be

$$s_{1,1}(t) = A \frac{\omega \sin\left(c\gamma_{1/2,1}t\right) - \sin \omega t}{\omega^2 - \left(c\gamma_{1/2,1}\right)^2}, \qquad (13)$$

where

$$A = \frac{4P_0}{\pi c\gamma_{1/2,1}b^2 J_{3/2}\left(\delta_{1/2,1}\right)^2} \int_0^b J_{1/2}\left(\frac{\delta_{1/2,1}}{b}r\right) r dr$$

and

$$u_{0,1}(t) = f_1 \cos\left(c\mu_{0,1}t\right) + B \frac{\omega \sin\left(c\mu_{0,1}t\right) - \sin \omega t}{\omega^2 - \left(c\mu_{0,1}\right)^2}, \quad (14)$$

where

$$B = \frac{2P_0}{c\mu_{0,1}b^2 \left(J_1\left(\lambda_{0,1}\right)\right)^2} \int_0^b J_0\left(\frac{\lambda_{0,1}}{b}r\right) r dr.$$

Hence, the model for simulation is

$$z(r, \theta, t) = \left(f_1 \cos\left(c\mu_{0,1}t\right) + B \frac{\omega \sin\left(c\mu_{0,1}t\right) - \sin \omega t}{\omega^2 - \left(c\mu_{0,1}\right)^2} \right)$$

$$\times J_0\left(\frac{\lambda_{0,1}}{b}r\right) + \left(A \frac{\omega \sin\left(c\gamma_{1/2,1}t\right) - \sin \omega t}{\omega^2 - \left(c\gamma_{1/2,1}\right)^2} \right)$$

$$\times J_{1/2}\left(\frac{\delta_{1,1}}{b}r\right) \sin \frac{1}{2}\theta \qquad (15)$$

and

$$z(r, t) = \sum_{m=1}^{\infty} A_{m1/2} J_{1/2}\left(\frac{\mu_{m1/2}}{b}r\right) \sin\left(\frac{\theta}{2}\right) \cos\left(\frac{\mu_{m1/2}v}{b}t\right)$$

$$+ \frac{4B_m J_0\left(\frac{\mu_m}{b}r\right)}{b^2 J_1^2\left(\mu_m\right)} \cos\left(\frac{\mu_m ct}{b}\right)$$

$$+ \frac{4C_m P_0 J_0\left(\frac{\mu_m}{b}r\right)}{\rho\mu_m b J_1^2\left(\mu_m\right)} \frac{\omega \sin\left(\frac{\mu_m ct}{b}\right) - \frac{\mu_m}{b}c\sin \omega t}{\omega^2 - \frac{\mu_m^2 c^2}{b^2}}, \qquad (16)$$

where

$$A_{m1/2} = \frac{2}{\pi b^2 J_{3/2}^2\left(\mu_{m1/2}\right)} \int_0^b \int_0^{2\pi} rF(r, \theta)$$

$$\times J_{1/2}\left(\frac{\mu_{m1/2}}{b}r\right) \sin\left(\frac{\theta}{2}\right) dr d\theta,$$

$$B_m = \int_0^b F(r) J_0\left(\frac{\mu_m}{b}r\right) r dr$$

and

$$C_m = \int_0^b J_0\left(\frac{\mu_m}{b}r\right) r dr.$$

Results of the simulation of (16) performed in MAPLE environment are shown in Figs. 2-4.

4. Discussion and conclusions

In this paper the vibratory patterns of the coupled system of the tympanum-malleus have been assessed by a simple numerical simulation.

The results of the simulation presented in Fig. 2 for the vibration mode (1,1) show an amplitude for the membrane larger than those for the handle of the malleus. The maximum amplitude obtained was around 1 μm, at a test frequency of 2 kHz (see Fig. 3). Also, Fig. 4 shows the level curves corresponding to the data in Fig. 2. It is important to emphasize that this frequency was chosen for the simulation because, as was demonstrated by Khanna and Tonndorf [23], the vibratory patterns of the TM remain essentially unchanged in their first mode up to a frequency of 2 kHz, with higher modes occurring above that value.

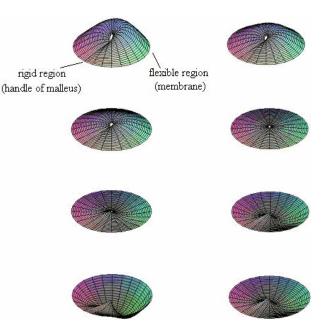rigid region (handle of malleus)   flexible region (membrane)

FIGURE 2. First mode of vibration of the TM obtained in MAPLE environment. An amplitude for the membrane (flexible region) larger than those for the handle of malleus (rigid region) is observed.
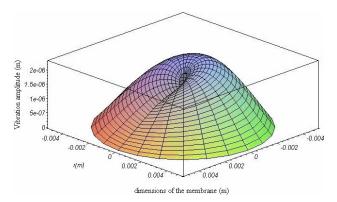
FIGURE 3. Maximum vibration amplitude for the TM ($\approx 1~\mu$m) at a test frequency of 2 kHz.
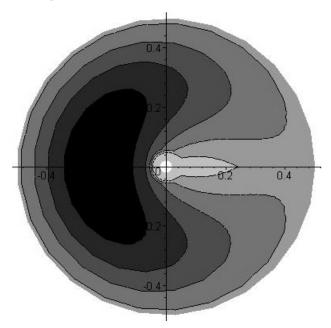

FIGURE 4. Level curves corresponding to the data shown in Fig. 2.

Our results for the vibrating amplitude are in reasonable agreement with several measurements reported in the literature. Rutten *et al.* [24], using a SQUID magnetometer, measured the displacement amplitude in the temporal bone of an isolated human ME. They found maximum values near 0.5 μm for the vibration amplitude, at frequencies of about 1 kHz, in response to a constant input sound level of 90 db SPL.

Very similar results were also reported by Sosa *et al.* [25,26], who performed TM vibration amplitude measurements on excised human temporal bones, by using a magnetic probe based on the measurements of the magnetic flux changes produced by the vibrations of a small magnet attached to the TM. They found maximum values near 0.5 μm for the TM vibration amplitude, at frequencies up to 1.5 kHz, in response to a constant input sound level of 100 db SPL.

On the other hand, in general, any pathology that affects the ME results in changes in the vibration amplitude of the TM. Otosclerosis, which is a fixation of the ossicular chain of the ME, results in a stiffening of the TM, and therefore in a decreasing of the displacement amplitude. On the other hand, a disarticulation of the ossicular joints results in an increase in compliance at the TM.

Finally, the numerical simulation can be easily handled to change input parameters, such as sound pressure on the TM and frequency, and also to introduce parameters that reflect different pathological conditions. Other situations such as the conical shape of the TM or some asymmetries could be easily considered.

Acknowledgments

∗ Corresponding author: Dr. Modesto Sosa, Physics Institute, University of Guanajuato, 37150 Leon, Gto., Mexico. Tel./Fax: (+52) 477-788-5100. e-mail: modesto@fisica.ugto.mx

1. R.Z. Gan, Q. Sun, R.K. Dyer, K.H. Chang, and K.J. Dormer, *Otol. Neurotol.* **23** (2002) 271.

2. R.Z. Gan, B. Feng, and Q. Sun, *Ann. Biomed. Eng.* **32** (2004) 847.

3. T. Koike, H. Wada, and T. Kobayashi, *J. Acoust. Soc. Am.* **111** (2002) 1306.

4. S.J. Daniel, W.R. Funnell, A.G. Zeitouni, M.D. Schloss, and J. Rappaport, *J Otolaryngol.* **30** (2001) 340.

5. W.R. Funnell and C. A. Laszlo, *J. Acoust. Soc. Am.* **63** (1978) 1461.

6. M. Bornitz, T. Zahnert, H. Hardtke, and K. Huttenbrink, *Audiol. Neurootol.* **4** (1999) 163.

7. J. Drescher, R. Schmidt, and H.J. Hardtke, *HNO.* **46** (1998) 129.

8. W.R. Funnell, *J. Acoust. Soc. Am.* **99** (1996) 3036.

9. W.R. Funnell, S.M. Khanna, and W.F. Decraemer, *J. Acoust. Soc. Am.* **91** (1992) 2082.

10. T. H. Lesser and K.R. Williams, *J. Laryngol. Otol.* **102** (1988) 209.

11. W.F. Decraemer and S.M. Khanna, *Hear. Res.* **72** (1994) 1.

12. M. Bance, D.P. Morris, R.G. Vanwijhe, M. Kiefte, and W.R. Funnell, *Otol. Neurotol.* **25** (2004) 903.

13. E. Gil-Carcedo, B. Perez-Lopez, L.A. Vallejo, L.M. Gil-Carcedo, and F. Montoya, *Acta Otorrinolaringol. Esp.* **53** (2002) 527.

14. W.F. Decraemer, J.J. Dirckx, and W.R. Funnell, *Hear. Res.* **51** (1991) 107.

15. A. Bhide, *J. Laryngol. Otol.* **106** (1992) 878.

16. M. von Unge, D. Bagger-Sjoback, and E. Borg, *Am. J. Otol.* **12** (1991) 407.

17. M.R. Stinson and S.M. Khanna, *J. Acoust. Soc. Am.* **85** (1989) 2481.

18. S.E. Voss, J.J. Rosowski, S.N. Merchant, and W.T. Peake, *Hear. Res.* **150** (2000) 43.

19. S. Puria and J.B. Allen, *J. Acoust. Soc. Am.* **104** (1998) 3463.

20. R.L. Goode, M. Killion, K. Nakamura, and S. Nishihara, *Am. J. Otol.* **15** (1994) 145.

21. M.E. Lutman and M. Martin, *J. Sound Vibration* **64** (1979) 133.

22. B. Feng and R.Z. Gan, *Biomechanics Modeling Mechanobiology* **3** (2004) 33.

23. S.M. Khanna and J. Tonndorf, *J. Acoust. Soc. Am.* **51** (1972) 1904.

24. W.L.C. Rutten *et al.*, *Cryogenics.* **2** (1982) 457.

25. M. Sosa, A.A.O. Carneiro, J.F. Colafemina, and O. Baffa, *J. Magn. Magn. Materials.* **226** (2001) 2067.

26. M. Sosa, A.A.O. Carneiro, O. Baffa, and J.F. Colafemina, *Rev. Sci. Instr.* **73** (2002) 3695.